phosphorylation. We therefore examined whether JNK activation enhances Jun ubiquitination by modulating the activity of Itch. Itch undergoes self-ubiquitination, and this activity was enhanced if it was isolated from WT T cells activated with antibodies to CD3 and CD28 (Fig. 3E). Little enhancement of Itch self-ubiquitination was observed after activation of *Mekk1*$^{\Delta KD}$ T cells (Fig. 3E). The ability of Itch to promote ubiquitination of a glutathione *S*-transferase (GST)–c-Jun substrate was enhanced in response to T cell activation and this response was also diminished in *Mekk1*$^{\Delta KD}$ cells (Fig. 3F). Both Itch self-ubiquitination and its ability to promote c-Jun polyubiquitination largely depended on incubation with both E1 and E2 (Ubc7) enzymes (fig. S6) and were reduced in activated T cells that were treated with a JNK inhibitor (Fig. 3G).

To examine whether Itch is a target for JNK-mediated phosphorylation, we separated proteins from nonactivated and activated T cells by two dimensional (2D) gel electrophoresis and transferred them to membranes. Following T cell activation, Itch became more negatively charged and displayed a lower isoelectric point (Fig. 4A). These changes are consistent with increased Itch phosphorylation and were reversed by calf intestine alkaline phosphatase (CIAP) (Fig. 4B). The kinetics of Itch phosphorylation correlated with those of JNK activation (fig. S7). Furthermore, when Itch phosphorylation was reduced by treatment with a JNK inhibitor and compared with that of WT cells, less TCR-induced Itch phosphorylation was observed in *Mekk1*$^{\Delta KD}$ cells (Fig. 4A). Similarly, Itch self-ubiquitination and c-Jun polyubiquitination were reduced after CIAP treatment of isolated Itch (Fig. 4C) (*21*). Moreover, incubation of Itch from nonstimulated T cells with activated JNK1 enhanced its self-ubiquitination, but incubation with inactive JNK1 had no effect (Fig. 4D). Incubation of Itch with active JNK1 also led to its efficient phosphorylation (Fig. 4E). Incubation of in vitro translated Itch with JNK1 also increased its self-ubiquitination and its ability to promote c-Jun polyubiquitination (Fig. 4F). Similar results were obtained with recombinant Itch produced in *Escherichia coli* (Fig. 4G). Consistent with the changes in c-Jun and JunB expression seen in *Jnk1*$^{-/-}$ and *Jnk2*$^{-/-}$ T cells (fig. S4), JNK1 is a more efficient Itch kinase than JNK2 and as a result is a more potent activator of Itch (fig. S8). The highly efficient phosphorylation of Itch by JNK1 is due to the presence of a JNK docking site, whose mutational inactivation prevents Itch phosphorylation and activation by JNK1 (*21*).

Extracellular stimuli often affect ubiquitin-dependent proteolysis by inducible target protein phosphorylation, which confers recognition by F box–containing E3 ligases (*5*). Instead, the effect of JNK on Itch-dependent c-Jun and JunB polyubiquitination and turnover is exerted by means of Itch itself. Some members of the HECT domain family are thought to be constitutively active E3 ligases. However, Itch catalytic activity is strongly modulated in response to T cell activation, through JNK-dependent phosphorylation. It is plausible that other members of the HECT domain family may be subject to similar regulation. The regulation is exerted at the level of the enzyme and not the substrate, and as is the case for F box-containing ligases, it allows a simultaneous increase in the turnover of multiple proteins. Disruption of Itch-dependent JunB turnover either through inactivation of Itch or inhibition of JNK results in increased expression of Th2 cytokine genes. Given the importance of JunB for *IL-4* gene transcription and Th2 differentiation (*12*, *13*), one function of JNK-dependent Itch activation is likely to be attenuation of IL-4 production in response to strong T cell activating signals.

References and Notes

1. A. Varshavsky, *Nature Cell Biol.* **5**, 373 (2003).
2. A. Hershko, A. Ciechanover, *Annu. Rev. Biochem.* **67**, 425 (1998).
3. C. M. Pickart, *Annu. Rev. Biochem.* **70**, 503 (2001).
4. M. Karin, Y. Ben-Neriah, *Annu. Rev. Immunol.* **18**, 621 (2000).
5. P. K. Jackson, A. G. Eldridge, *Mol. Cell* **9**, 923 (2002).
6. M. Karin, *J. Biol. Chem.* **270**, 16483 (1995).
7. S. Gupta *et al.*, *EMBO J.* **15**, 2760 (1996).
8. A. M. Musti, M. Treier, D. Bohmann, *Science* **275**, 400 (1997).
9. S. Y. Fuchs, L. Dolan, R. J. Davis, Z. Ronai, *Oncogene* **13**, 1531 (1996).
10. A. S. Nateri, L. Riera-Sans, C. Da Costa, A. Behrens, *Science* **303**, 1374 (2004).
11. D. Fang *et al.*, *Nature Immunol.* **3**, 281 (2002).
12. B. Li, C. Tournier, R. J. Davis, R. A. Flavell, *EMBO J.* **18**, 420 (1999).
13. B. Hartenstein *et al.*, *EMBO J.* **21**, 6321 (2002).
14. C. Dong *et al.*, *Science* **282**, 2092 (1998).
15. C. Dong *et al.*, *Nature* **405**, 91 (2000).
16. L. Zhang *et al.*, *EMBO J.* **22**, 4443 (2003).
17. A. Minden *et al.*, *Science* **266**, 1719 (1994).
18. W. E. Paul, R. A. Seder, *Cell* **76**, 241 (1994).
19. K. M. Murphy *et al.*, *Annu. Rev. Immunol.* **18**, 451 (2000).
20. C. S. Hsieh, S. E. Macatonia, A. O'Garra, K. M. Murphy, *J. Exp. Med.* **181**, 713 (1995).
21. M. Gao, M. Karin, unpublished data.
22. K. Sabapathy *et al.*, *J. Exp. Med.* **193**, 317 (2001).
23. B. L. Bennett *et al.*, *Proc. Natl. Acad. Sci. U.S.A.* **98**, 13681 (2001).
24. T. Kallunki, T. Deng, M. Hibi, M. Karin, *Cell* **87**, 929 (1996).
25. T. Borsello *et al.*, *Nature Med.* **9**, 1180 (2003).
26. T. Smeal, B. Binetruy, D. A. Mercola, M. Birrer, M. Karin, *Nature* **354**, 494 (1991).
27. We thank A. Lin for providing the JNKK2-JNK1 fusion proteins and D. Bohmann for Jun^{Ala} construct. We thank A. Ciechanover and T. Hunter for helpful discussion and critique and L. Chang and J. Park for assistance. M.G. was supported by a postdoctoral fellowship from the Damon Runyon Cancer Research Foundation. T.L. was supported by the Alfred Benzon Foundation and the LEO Pharma Research Foundation, Denmark. Work was supported by the Sandler Family Research Foundation and NIH grants AI43477, ES04151 and ES06376 to M.K. and by NIH grant R21AI48542 and a Research Scholar grant from the American Cancer Society (ACS) to Y.-C.L. M.K. is the Frank and Else Schilling ACS Research Professor.

Supporting Online Material

www.sciencemag.org/cgi/content/full/1099414/DC1
Materials and Methods
Figs. S1 to S8
References

21 April 2004; accepted 18 August 2004
Published online 9 September 2004;
10.1126/science.1099414
Include this information when citing this paper.

Downloaded from https://www.science.org at University of California Santa Barbara on June 05, 2025

A Glycine-Dependent Riboswitch That Uses Cooperative Binding to Control Gene Expression

Maumita Mandal,[1] Mark Lee,[2] Jeffrey E. Barrick,[2] Zasha Weinberg,[3] Gail Mitchell Emilsson,[1] Walter L. Ruzzo,[3,4] Ronald R. Breaker[1]*

We identified a previously unknown riboswitch class in bacteria that is selectively triggered by glycine. A representative of these glycine-sensing RNAs from *Bacillus subtilis* operates as a rare genetic on switch for the *gcvT* operon, which codes for proteins that form the glycine cleavage system. Most glycine riboswitches integrate two ligand-binding domains that function cooperatively to more closely approximate a two-state genetic switch. This advanced form of riboswitch may have evolved to ensure that excess glycine is efficiently used to provide carbon flux through the citric acid cycle and maintain adequate amounts of the amino acid for protein synthesis. Thus, riboswitches perform key regulatory roles and exhibit complex performance characteristics that previously had been observed only with protein factors.

Genetic control by riboswitches located within the noncoding regions of mRNAs is widespread among bacteria (*1*–*3*). About 2% of the genes in *Bacillus subtilis* are regulated by these metabolite-binding RNA domains (*4*). All riboswitches discovered thus far use

a single highly structured aptamer as a sensor for their corresponding target molecules. Selective binding of metabolite by the aptamer causes allosteric modulation of the secondary and tertiary structures of the mRNA 5′-untranslated region (5′-UTR), which changes gene expression by one or more mechanisms that influence transcription termination (*5*, *6*), translation initiation (*7*, *8*), or mRNA processing (*9*, *10*).

The existence of riboswitches in modern cells implies that RNA molecules have considerable potential for forming intricate structures that are comparable to protein receptors. Furthermore, riboswitches do not have an obligate need for additional protein factors to carry out their gene control tasks and thus serve as economical genetic switches that sense and respond to changes in metabolite concentrations. However, higher-ordered functions exhibited by some protein factors have not been observed with natural riboswitches. For example, many protein enzymes, receptors, and gene control factors make use of cooperative binding to provide the cell with a means to rapidly respond to small changes in ligand concentrations [e.g., (*11*–*13*)].

We recently reported the identification of highly conserved RNA motifs in numerous bacterial species that have features similar to known riboswitches (*14*). One of these motifs, termed *gcvT* (Fig. 1A), is found in many bacteria, where it typically resides upstream of genes that express protein components of the glycine cleavage system. In *B. subtilis*, a three-gene operon (*gcvT-gcvPA-gcvPB*) codes for components of this protein complex, which catalyzes the initial reactions for use of glycine as an energy source (*15*, *16*).

Two forms of the *gcvT* RNA motif, type I and type II (Fig. 1A), had been identified on the basis of differences in the sequences that flank their conserved cores (*14*). More sensitive computational scans (*17*) revealed that both motif types reside adjacent to each other, as represented by the architecture of the region immediately upstream of the *VC1422* gene (a putative sodium and alanine symporter) from *Vibrio cholerae* (Fig. 1B). Individually, the type I and type II elements appear to represent separate aptamer domains, wherein each presumably binds a separate target molecule. Furthermore, the linker sequence between the two aptamers exhibits some conservation of both sequence and length, suggesting that the aptamers are functionally coupled (fig. S1).

The metabolite-binding capabilities of *V. cholerae* RNAs were assessed by using a

[1]Department of Molecular, Cellular, and Developmental Biology, [2]Department of Molecular Biophysics and Biochemistry, Yale University, Post Office Box 208103, New Haven, CT 06520–8103, USA. [3]Department of Computer Science and Engineering, [4]Department of Genome Sciences, University of Washington, Post Office Box 352350, Seattle, WA 98195, USA.

*To whom correspondence should be addressed. E-mail: ronald.breaker@yale.edu

Downloaded from https://www.science.org at University of California Santa Barbara on June 05, 2025

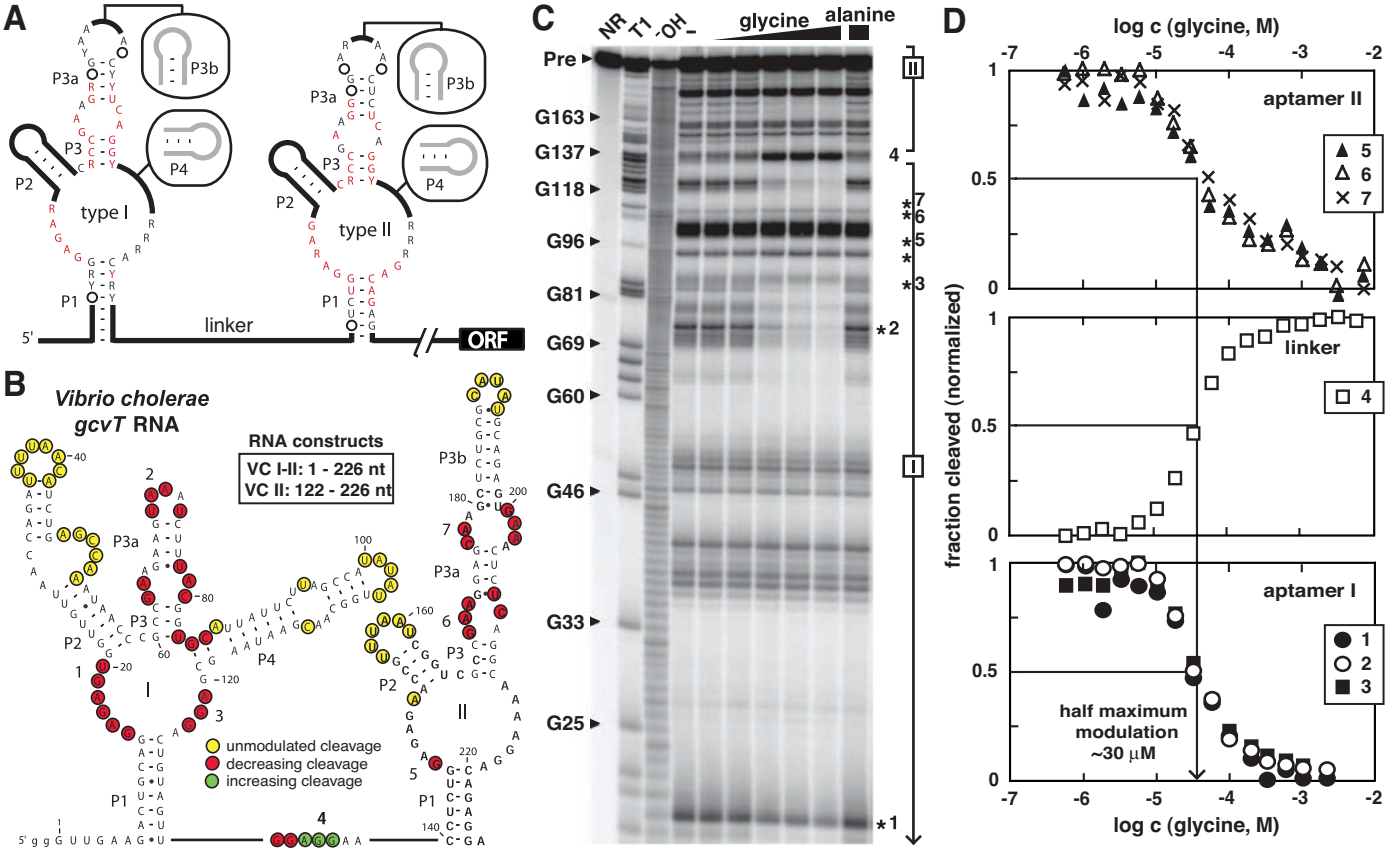

Fig. 1. Type I and type II *gcvT* motifs are natural RNA aptamers for glycine. (**A**) Consensus nucleotides present in more than 80% (black) and 95% (red) of representative sequences were identified by bioinformatics (*17*) (fig. S1). Circles and thick lines represent nucleotides whose base identities are not conserved. P1 through P4 identify common base-paired elements. ORF, open reading frame. (**B**) Patterns of spontaneous cleavage that occur with VC I-II in the absence and presence of glycine are depicted. Numbers adjacent to sites of changing spontaneous cleavage correspond to gel bands denoted with asterisks in (C) and data sets in (D). (**C**) Spontaneous cleavage products of VC I-II upon separation by polyacrylamide gel electrophoresis (PAGE) (*7*, *8*) (fig. S2). NR, T1, and $^{-}$OH represent no reaction, partial digest with RNase T1, and partial digest with alkali, respectively. Pre, precursor RNA. Some fragment bands corresponding to T1 digestion (cleaves after G residues) are labeled. Numbered asterisks identify locations of major structural modulation in response to glycine. The two rightmost lanes carry 1 mM of the amino acids noted. Brackets labeled I and II identify RNA fragments that correspond to cleavage events in the type I and type II aptamers, respectively. (**D**) Plots of the extent of spontaneous cleavage products versus increasing concentrations of glycine for aptamer I (sites 1 through 3), aptamer II (sites 5 through 7), and the linker sequence (site 4). C, concentration.

method termed inline probing (*18*), which can reveal metabolite-induced changes in aptamer structure by monitoring changes in the levels of spontaneous RNA cleavage (*4*, *6*, *7*–*9*). For example, the addition of glycine at 1 mM caused changes in the pattern of spontaneous cleavage of a 226-nucleotide RNA construct (VC I-II) that carries both aptamer types (Fig. 1C), whereas 1 mM L-alanine did not induce change.

Similar results were observed when a 105-nucleotide RNA (VC II) carrying the type II aptamer alone was used for inline probing (fig. S2). Because both type I and type II domains undergo similar structural changes upon introduction of glycine and because VC II alone exhibits ligand-dependent structural change, we conclude that each domain serves as a separate glycine binding aptamer. Furthermore, all three sections of the VC I-II construct (aptamer I, linker, and aptamer II) responded to glycine equally at various concentrations (Fig. 1D). This concerted response to glycine suggests the two aptamers either have perfectly matched affinities for glycine or bind glycine in a highly cooperative manner.

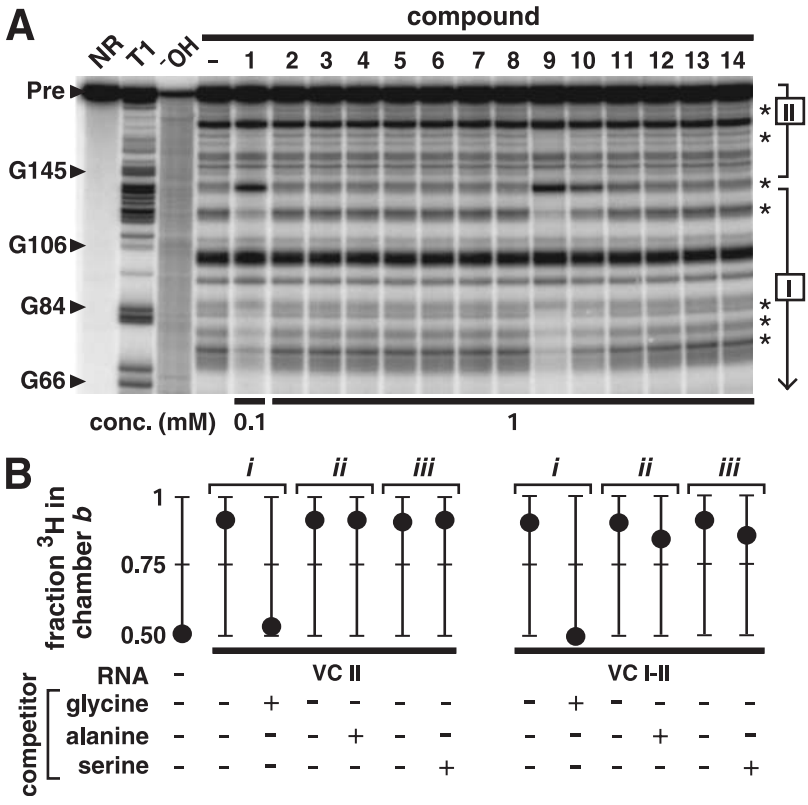

Fig. 2. Ligand specificity of VC II and VC I-II RNAs. (**A**) Inline probing of VC I-II in the absence (–) or presence of glycine (compound 1) or the analogs L-alanine (2), D-alanine (3), L-serine (4), L-threonine (5), sarcosine (6), mercaptoacetic acid (7), β-alanine (8), glycine methyl ester (9), glycine tert-butyl ester (10), glycine hydroxamate (11), glycinamide (12), aminomethane sulfonic acid (13), and glycyl-glycine (14). Other notations are as described in the legend to Fig. 1C. (**B**) Equilibrium dialysis data for VC II and VC I-II (100 μM) in the absence (–) or presence (+) of excess (1 mM) unlabeled glycine, alanine, or serine as indicated. Fraction of ^{3}H-glycine in chamber b reflects the amount of glycine bound by RNA plus half the total amount of free glycine in chambers a and b versus the total amount of ^{3}H-glycine. *i* to *iii*, separate experiments where RNA and ^{3}H are equilibrated (left) and competitor is subsequently added.

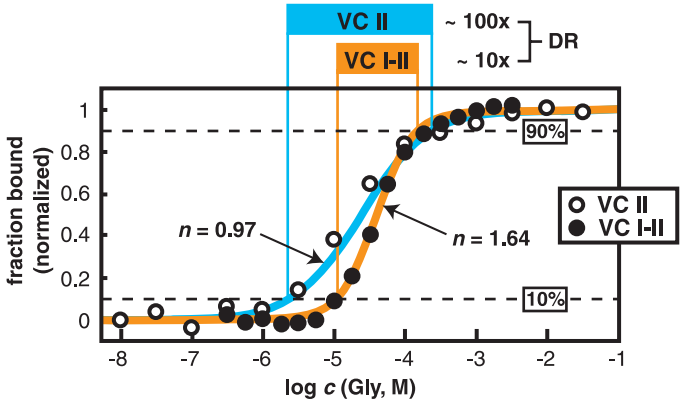

Fig. 3. Cooperative binding of two glycine molecules by the VC I-II RNA. Plot depicts the fraction of VC II (open) and VC I-II (solid) bound to ligand versus the concentration of glycine. The constant, *n*, is the Hill coefficient for the lines as indicated that best fit the aggregate data from four different regions (fig. S3). Shaded boxes demark the dynamic range (DR) of glycine concentrations needed by the RNAs to progress from 10%- to 90%-bound states.

The molecular recognition specificity of VC I-II was examined by using inline probing with a variety of glycine analogs. The RNA exhibited measurable structural modulation with the methyl ester and tertiary butyl ester analogs of glycine but rejected all other analogs when tested at 1 mM (Fig. 2A). The concentrations of ligand needed to cause half-maximal structure modulation of VC II are about 10 μM for glycine, 100 μM for glycine methyl ester, 1 mM for glycine tertiary butyl ester, and 1 mM for glycine hydroxamate (*19*). Specificity for glycine also was observed by using equilibrium dialysis. For example, when an equilibrium dialysis system is preequilibrated with either VC II or VC I-II RNAs, excess glycine restored an equal distribution of ^{3}H-glycine upon subsequent incubation (Fig. 2B). However, the addition of either L-alanine or L-serine failed to restore equal distribution, confirming that the RNAs serve as precise sensors for glycine.

We explored the stoichiometry of glycine binding to these RNAs by using equilibrium dialysis with high glycine concentrations. When three equivalents of the amino acid were present versus one equivalent of VC II RNA (100 μM), we observed a shift in glycine distribution (*19*) that indicates ~0.8 equivalents (1 expected) of glycine were bound by RNA. In contrast, when one equivalent of the VC I-II RNA was present (two aptamer equivalents), there is a ~1.6-fold increase (2 expected) in the amount of glycine that was bound by RNA. These data provide preliminary evidence for a stoichiometry of 1:1 between glycine and each individual aptamer.

Our laboratory created an engineered allosteric RNA construct with a tandem aptamer configuration that demonstrated cooperative binding of multiple ligands (*20*), thus providing a precedent for this more sophisticated form of RNA switch. If the two aptamers of VC I-II function cooperatively, then structural changes in the RNA should be atypically responsive to increasing glycine concentrations compared with those of a single glycine aptamer. The ligand-dependent modulation of VC II structure by glycine (Fig. 3) was typical of that observed for single aptamer domains of known riboswitches (*4*, *6*–*9*, *21*–*24*). The

Downloaded from https://www.science.org at University of California Santa Barbara on June 05, 2025

change from ~10% to ~90% ligand-bound VC I RNA occurred over a ~100-fold increase in glycine concentration, which corresponds with the response predicted for a receptor that binds a single ligand (fig. S3).

In contrast, VC I-II underwent the same change in ligand occupancy over only a ~10-fold increase in glycine concentration (Fig. 3). This reduction in the dynamic range for the glycine-mediated response is consistent with the hypothesis that glycine binding at one site substantially improves the affinity for glycine binding to the other site. The Hill coefficient (*25*, *26*) calculated for VC I-II is 1.64, whereas the maximum value for two binding sites is 2. In comparison, the Hill coefficient for the oxygen-carrying protein hemoglobin is 2.8 (*27*), whereas the maximum value for four binding sites is 4. Thus, the degree of cooperativity per binding site with the two VC I-II aptamers is equal to or greater than that derived for each of the four sites in hemoglobin.

A cooperative mechanism for ligand binding is further supported by the observation that single-point mutations made to either of the conserved cores of VC I-II cause substantial loss of glycine-binding affinity to the mutated aptamer and also cause a dramatic loss of affinity to the unaltered aptamer (fig. S4). Thus, the binding of glycine at one site induces the adjacent site to exhibit an improvement in ligand binding affinity by ~100- to ~1000-fold.

Tandem aptamer architecture (Fig. 4A) and selective glycine recognition (*19*) are also observed with RNA corresponding to the putative 5′-UTR of the *gcvT* operon from *B. subtilis*. This provided us with a construct that is more amenable to experiments that assess whether the *gcvT* RNA is important for genetic control. We used single-round transcription assays (*17*) to determine whether a DNA construct corresponding to the intergenic region (IGR) upstream of the *B. subtilis gcvT* operon yields transcripts whose termination sites are influenced by glycine. In the absence of glycine, only ~30% of the RNA products generated by in vitro transcription were full-length (Fig. 4B). The remaining ~70% were premature termination products that correspond in length to that expected if RNA polymerase stalls at a putative intrinsic terminator (*28*, *29*) that partially overlaps the second glycine aptamer (also fig. S5).

The addition of glycine caused a substantial increase in the amount of full-length RNA transcript relative to the amount of truncated RNA (Fig. 4B). This improvement is induced only by glycine or by other analogs that cause RNA structure modulation. Compounds such as serine, alanine, and other analogs that do not induce modulation also failed to trigger an increase in the production of full-length transcripts (fig. S5) (*19*).

Furthermore, the glycine-dependent increase in the yield of full-length transcripts corresponded with that expected for a cooperative RNA switch requiring two ligand binding events. Fitting the transcription data yields a curve that corresponded to cooperative ligand binding, with a Hill coefficient of 1.4 (Fig. 4B). Therefore, transcription control by

Downloaded from https://www.science.org at University of California Santa Barbara on June 05, 2025

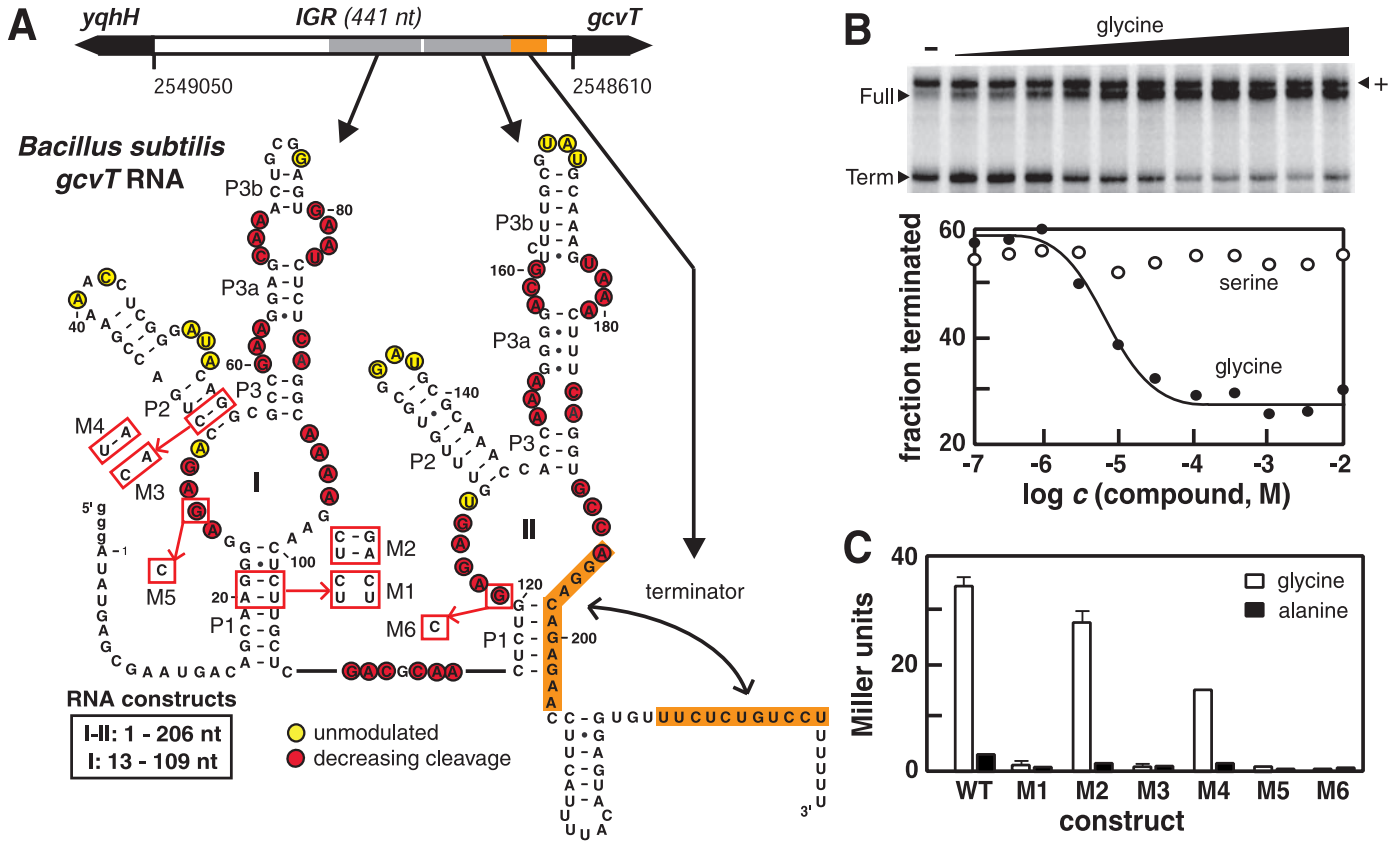

Fig. 4. Control of *B. subtilis gcvT* RNA expression in vitro and in vivo. (**A**) The IGR between the *yqhH* and *gcvT* genes of *B. subtilis* encompassing both aptamers I and II was used for in vitro transcription and in vivo expression assays. Inline probing results were mapped, and mutations used to assess riboswitch function are indicated with red boxes. Orange shading identifies the putative intrinsic terminator stem, which is expected to exhibit mutually exclusive formation of aptamer II when bound to glycine. nt, nucleotide. (**B**) Single-round in vitro transcription assays demonstrating that full-length (Full) transcripts are favored when >10 μM glycine is added to the transcription mixture, whereas serine and most glycine analogs (fig. S5) are rejected by the riboswitch. The line reflects a best-fit curve to an equation reflecting cooperative binding with a Hill coefficient of 1.4 (*19*). An additional transcription product, termed "+," appears to be due to spurious transcription initiation (*17*). (**C**) Plot of the expression of a β-galactosidase reporter gene fused to wild-type (WT) *gcvT* IGR or to a series of mutant IGRs (M1–M6). Data reflect the averages of three assays with two replicates each. Error bars indicate ± two standard deviations.

the *gcvT* 5′-UTR of *B. subtilis* responds to glycine with characteristics that parallel those observed when conducting inline probing of the cooperative VC I-II RNA.

To assess whether glycine binding and in vitro transcription control correspond to genetic control events in vivo, we generated reporter constructs by fusing the IGR upstream of the *gcvT* operon from *B. subtilis* to a β-galactosidase reporter gene and integrated them into the bacterial genome (*17*). The reporter fusion construct carrying the wild-type IGR expresses a high amount of β-galactosidase when glycine is present in the growth medium, whereas a low amount of gene expression results when alanine is present (Fig. 4C). These results indicate that the *gcvT* motif is part of a glycine-responsive riboswitch with a default state that is off. Glycine binding is required to activate gene expression, as was also observed with the in vitro transcription assays (Fig. 4B).

The importance of several conserved features of the motif were examined by mutating the P1 and P2 stems of the first aptamer domain to disrupt (variants M1 and M3, respectively) and restore (M2 and M4, respectively) base pairing (Fig. 4A). Resulting gene expression levels from constructs carrying the mutant IGRs are consistent with base-paired elements predicted from phylogenetic analyses (*14*) (fig. S1). Furthermore, the introduction of mutations into the conserved cores of either aptamer I or aptamer II (variants M5 and M6, respectively) caused a complete loss of reporter gene activation. This latter result suggests that glycine binding to both aptamers is necessary to trigger gene activation, which is consistent with a model wherein cooperative glycine binding is important for riboswitch function.

The glycine-dependent riboswitch is a remarkable genetic control element for several reasons. First, glycine riboswitches form selective binding pockets for a ligand composed of only 10 atoms and thus bind the smallest organic compound among known natural and engineered RNA aptamers. This observation is consistent with the hypothesis that RNA has sufficient structural potential to selectively bind a wide range of biomolecules.

Second, the 5′-UTR of the *B. subtilis gcvT* operon is a genetic on switch, and thus joins the adenine riboswitch (*23*) as a rare type of RNA that has been proven to harness ligand binding and activate gene expression. In most instances, riboswitches cause repression of their associated genes, which is to be expected because many of these genes are involved in biosynthesis or import of the target metabolites. However, the glycine riboswitch from *B. subtilis* controls the expression of three genes required for glycine degradation. A ligand-activated riboswitch would be required to determine whether sufficient amino acid substrate is present to warrant production of the glycine cleavage system, thereby providing a rationale for why this rare on switch is used.

Third, this is the only known metabolite-binding riboswitch class that regularly makes use of a tandem aptamer configuration. In both *V. cholerae* and *B. subtilis*, the juxtaposition of aptamers enables the cooperative binding of two glycine molecules. For the *B. subtilis* riboswitch, this characteristic is expected to result in unusually rapid activation and repression of genes encoding the glycine cleavage system in response to rising and falling concentrations of glycine, respectively. Given the prevalence of the tandem architecture of glycine riboswitches, this more "digital" switch likely gives the bacterium an important selective advantage by controlling gene expression in response to small changes in glycine.

References and Notes

1. W. C. Winkler, R. R. Breaker, *ChemBioChem* **4**, 1024 (2003).
2. A. G. Vitreschak, D. A. Rodionov, A. A. Mironov, M. S. Gelfand, *Trends Genet.* **20**, 44 (2004).
3. E. Nudler, A. S. Mironov, *Trends Biochem. Sci.* **29**, 11 (2004).
4. M. Mandal, B. Boese, J. E. Barrick, W. C. Winkler, R. R. Breaker, *Cell* **113**, 577 (2003).
5. A. S. Mironov *et al.*, *Cell* **111**, 747 (2002).
6. W. C. Winkler, S. Cohen-Chalamish, R. R. Breaker, *Proc. Natl. Acad. Sci. U.S.A.* **99**, 15908 (2002).
7. A. Nahvi *et al.*, *Chem. Biol.* **9**, 1043 (2002).
8. W. Winkler, A. Nahvi, R. R. Breaker, *Nature* **419**, 952 (2002).
9. N. Sudarsan, J. E. Barrick, R. R. Breaker, *RNA* **9**, 644 (2003).
10. W. C. Winkler, A. Nahvi, A. Roth, J. A. Collins, R. R. Breaker, *Nature* **428**, 281 (2004).
11. M. Ptashne, A. Gann, *Genes & Signals* (Cold Spring Harbor Press, Cold Spring Harbor, NY, 2002).
12. B. I. Kurganov, *Allosteric Enzymes* (Wiley, New York, 1978).
13. A. A. Antson *et al.*, *Nature* **374**, 693 (1995).
14. J. F. Barrick *et al.*, *Proc. Natl. Acad. Sci. U.S.A.* **101**, 6421 (2004).
15. G. Kikuchi, *Mol. Cell. Biochem.* **1**, 169 (1973).
16. R. Duce, J. Bourguignon, M. Neuburger, F. Rébeillé, *Trends Plant Sci.* **6**, 167 (2001).
17. Materials and methods are available on *Science* Online.
18. G. A. Soukup, R. R. Breaker, *RNA* **5**, 1308 (1999).
19. M. Mandal *et al.*, unpublished data.
20. A. M. Jose, G. A. Soukup, R. R. Breaker, *Nucleic Acids Res.* **29**, 1631 (2001).
21. W. C. Winkler, A. Nahvi, N. Sudarsan, J. E. Barrick, R. R. Breaker, *Nature Struct. Biol.* **10**, 701 (2003).
22. N. Sudarsan, J. K. Wickiser, S. Nakamura, M. S. Ebert, R. R. Breaker, *Genes Dev.* **17**, 2688 (2003).
23. M. Mandal, R. R. Breaker, *Nature Struct. Mol. Biol.* **11**, 29 (2004).
24. A. Nahvi, J. E. Barrick, R. R. Breaker, *Nucleic Acids Res.* **32**, 143 (2004).
25. A. V. Hill, *J. Physiol.* **40**, iv (1910).
26. M. Weissbluth, in *Molecular Biology Biochemistry and Biophysics*, A. Kleinzeller, Ed. (Springer-Verlag, New York, 1974), vol. 15, pp. 27–41.
27. S. J. Edelstein, *Annu. Rev. Biochem.* **44**, 209 (1975).
28. I. Gusarov, E. Nudler, *Mol. Cell* **3**, 495 (1999).
29. W. S. Yarnell, J. W. Roberts, *Science* **284**, 611 (1999).

30. We thank members of the Breaker laboratory for helpful discussions and G. Reguera and B. Bassler for providing genomic DNA for *V. cholerae*. This work was supported by grants from the NIH and the NSF. R.R.B. is also grateful for support from the Yale Liver Center and the David and Lucile Packard Foundation.

Supporting Online Material

www.sciencemag.org/cgi/content/full/306/5694/275/DC1
Materials and Methods
Figs. S1 to S5

27 May 2004; accepted 24 August 2004

Human PAD4 Regulates Histone Arginine Methylation Levels via Demethylimination

Yanming Wang,[1,2] Joanna Wysocka,[1,2] Joyce Sayegh,[3] Young-Ho Lee,[4] Julie R. Perlin,[1] Lauriebeth Leonelli,[1] Lakshmi S. Sonbuchner,[1] Charles H. McDonald,[5] Richard G. Cook,[5] Yali Dou,[6] Robert G. Roeder,[6] Steven Clarke,[3] Michael R. Stallcup,[4] C. David Allis,[2]* Scott A. Coonrod[1]*

Methylation of arginine (Arg) and lysine residues in histones has been correlated with epigenetic forms of gene regulation. Although histone methyltransferases are known, enzymes that demethylate histones have not been identified. Here, we demonstrate that human peptidylarginine deiminase 4 (PAD4) regulates histone Arg methylation by converting methyl-Arg to citrulline and releasing methylamine. PAD4 targets multiple sites in histones H3 and H4, including those sites methylated by coactivators CARM1 (H3 Arg^{17}) and PRMT1 (H4 Arg^{3}). A decrease of histone Arg methylation, with a concomitant increase of citrullination, requires PAD4 activity in human HL-60 granulocytes. Moreover, PAD4 activity is linked with the transcriptional regulation of estrogen-responsive genes in MCF-7 cells. These data suggest that PAD4 mediates gene expression by regulating Arg methylation and citrullination in histones.

Posttranslational histone modifications, such as phosphorylation, acetylation, and methylation, regulate a broad range of DNA and chromatin-templated nuclear events, including transcription (*1–3*). Pairs of opposing enzymes, such as acetyltransferases-deacetylases

Downloaded from https://www.science.org at University of California Santa Barbara on June 05, 2025

ERRATUM

post date 26 November 2004

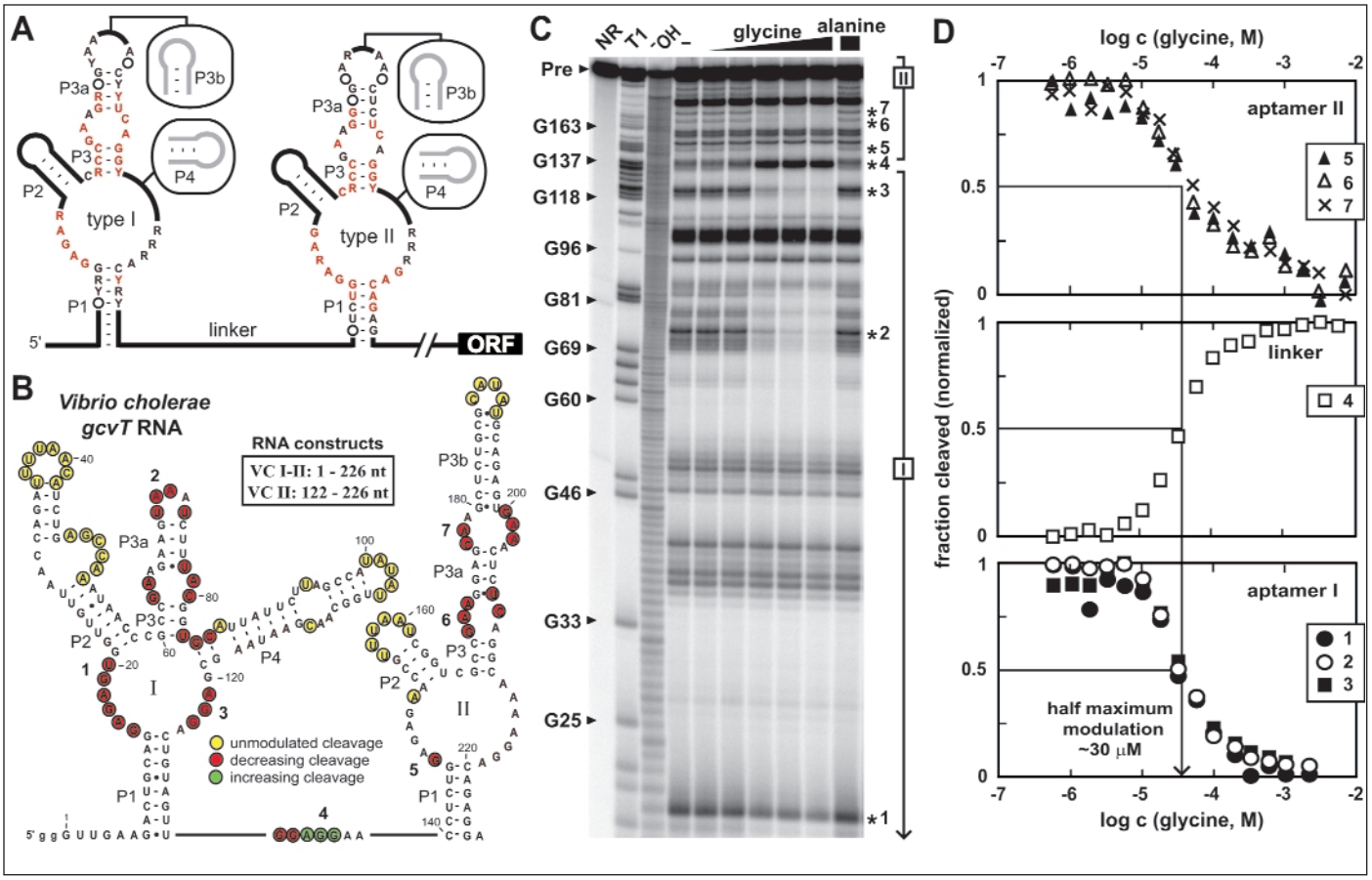

Reports: "A glycine-dependent riboswitch that uses cooperative binding to control gene expression" by M. Mandal *et al.* (8 Oct. 2004, p. 275). There was an error introduced into Fig. 1C during production. Several numbers and asterisks moved when the graphic was adjusted. The corrected figure is shown here.

Downloaded from https://www.science.org at University of California Santa Barbara on June 05, 2025